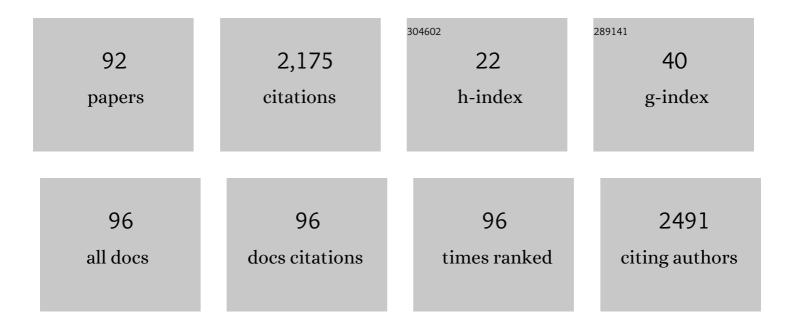
List of Publications by Year in descending order

Source: https://exaly.com/author-pdf/504368/publications.pdf Version: 2024-02-01



MENCSU ZENC

#	Article	IF	CITATIONS
1	Guidelines for the Diagnosis and Treatment of Hepatocellular Carcinoma (2019 Edition). Liver Cancer, 2020, 9, 682-720.	4.2	427
2	A Radiomics Nomogram for Preoperative Prediction of Microvascular Invasion in Hepatocellular Carcinoma. Liver Cancer, 2019, 8, 373-386.	4.2	201
3	CT radiomics may predict the grade of pancreatic neuroendocrine tumors: a multicenter study. European Radiology, 2019, 29, 6880-6890.	2.3	106
4	Consensus report from the 7th International Forum for Liver Magnetic Resonance Imaging. European Radiology, 2016, 26, 674-682.	2.3	86
5	Microvascular invasion in small hepatocellular carcinoma: Is it predictable with preoperative diffusionâ€weighted imaging?. Journal of Gastroenterology and Hepatology (Australia), 2014, 29, 330-336.	1.4	75
6	Differentiating between malignant and benign renal tumors: do IVIM and diffusion kurtosis imaging perform better than DWI?. European Radiology, 2019, 29, 6930-6939.	2.3	59
7	A radiomics-based biomarker for cytokeratin 19 status of hepatocellular carcinoma with gadoxetic acid–enhanced MRI. European Radiology, 2020, 30, 3004-3014.	2.3	53
8	Intravoxel incoherent motion diffusion-weighted imaging for the assessment of renal fibrosis of chronic kidney disease: A preliminary study. Magnetic Resonance Imaging, 2018, 47, 118-124.	1.0	51
9	Mild cognitive impairment in de novo Parkinson's disease: A neuromelanin MRI study in locus coeruleus. Movement Disorders, 2019, 34, 884-892.	2.2	49
10	Chronic kidney disease: Pathological and functional evaluation with intravoxel incoherent motion diffusionâ€weighted imaging. Journal of Magnetic Resonance Imaging, 2018, 47, 1251-1259.	1.9	46
11	Comparison of Biexponential and Monoexponential Model of Diffusion-Weighted Imaging for Distinguishing between Common Renal Cell Carcinoma and Fat Poor Angiomyolipoma. Korean Journal of Radiology, 2016, 17, 853.	1.5	42
12	Staging liver fibrosis with DWI: is there an added value for diffusion kurtosis imaging?. European Radiology, 2018, 28, 3041-3049.	2.3	42
13	Combined Visualization of Nigrosome-1 and Neuromelanin in the Substantia Nigra Using 3T MRI for the Differential Diagnosis of Essential Tremor and de novo Parkinson's Disease. Frontiers in Neurology, 2019, 10, 100.	1.1	39
14	Intramyocardial Hemorrhage and the "Wave Front―of Reperfusion Injury Compromising Myocardial Salvage. Journal of the American College of Cardiology, 2022, 79, 35-48.	1.2	38
15	Prediction of Microvascular Invasion in Hepatocellular Carcinoma via Deep Learning: A Multi-Center and Prospective Validation Study. Cancers, 2021, 13, 2368.	1.7	36
16	Neuromelanin-sensitive MRI of the substantia nigra: An imaging biomarker to differentiate essential tremor from tremor-dominant Parkinson's disease. Parkinsonism and Related Disorders, 2019, 58, 3-8.	1.1	35
17	Combined hepatocellular-cholangiocarcinoma: which preoperative clinical data and conventional MRI characteristics have value for the prediction of microvascular invasion and clinical significance?. European Radiology, 2020, 30, 5337-5347.	2.3	35
18	Liver Computed Tomographic Perfusion in the Assessment of Microvascular Invasion in Patients With Small Hepatocellular Carcinoma. Investigative Radiology, 2015, 50, 188-194.	3.5	33

#	Article	IF	CITATIONS
19	Histological Subtypes Classification of Lung Cancers on CT Images Using 3D Deep Learning and Radiomics. Academic Radiology, 2021, 28, e258-e266.	1.3	32
20	Assessing EGFR gene mutation status in non-small cell lung cancer with imaging features from PET/CT. Nuclear Medicine Communications, 2019, 40, 842-849.	0.5	30
21	MRI features predict microvascular invasion in intrahepatic cholangiocarcinoma. Cancer Imaging, 2020, 20, 40.	1.2	27
22	Peritumoral Dilation Radiomics of Gadoxetate Disodium-Enhanced MRI Excellently Predicts Early Recurrence of Hepatocellular Carcinoma without Macrovascular Invasion After Hepatectomy. Journal of Hepatocellular Carcinoma, 2021, Volume 8, 545-563.	1.8	26
23	ADC <sub>total</sub> ratio and D ratio derived from intravoxel incoherent motion early after TACE are independent predictors for survival in hepatocellular carcinoma. Journal of Magnetic Resonance Imaging, 2017, 46, 820-830.	1.9	24
24	Pathological assessment of chronic kidney disease with <scp>DWI</scp> : Is there an added value for diffusion kurtosis imaging?. Journal of Magnetic Resonance Imaging, 2021, 54, 508-517.	1.9	24
25	A predictive model integrating deep and radiomics features based on gadobenate dimeglumine-enhanced MRI for postoperative early recurrence of hepatocellular carcinoma. Radiologia Medica, 2022, 127, 259-271.	4.7	24
26	Microvascular invasion in hepatocellular carcinoma: is it predictable with a new, preoperative application of diffusion-weighted imaging?. Clinical Imaging, 2017, 41, 101-105.	0.8	22
27	Staging liver fibrosis in chronic hepatitis B with <i>T</i> <sub>1</sub> relaxation time index on gadoxetic acidâ€enhanced MRI: Comparison with aspartate aminotransferaseâ€toâ€platelet ratio index and FIBâ€4. Journal of Magnetic Resonance Imaging, 2017, 45, 1186-1194.	1.9	21
28	Differentiation of renal cell carcinoma subtypes with different iodine quantification methods using single-phase contrast-enhanced dual-energy CT: areal vs. volumetric analyses. Abdominal Radiology, 2018, 43, 672-678.	1.0	21
29	Prostate cancer aggressive prediction: preponderant diagnostic performances of intravoxel incoherent motion (IVIM) imaging and diffusion kurtosis imaging (DKI) beyond ADC at 3.0 T scanner with gleason score at final pathology. Abdominal Radiology, 2019, 44, 3441-3452.	1.0	20
30	Role of Myocardial Extracellular Volume Fraction Measured with Magnetic Resonance Imaging in the Prediction of Left Ventricular Functional Outcome after Revascularization of Chronic Total Occlusion of Coronary Arteries. Korean Journal of Radiology, 2019, 20, 83.	1.5	18
31	Comparison of the effect of region-of-interest methods using gadoxetic acid-enhanced MR imaging with diffusion-weighted imaging on staging hepatic fibrosis. Radiologia Medica, 2016, 121, 821-827.	4.7	15
32	Comparison of gadoxetic acid versus gadopentetate dimeglumine for the detection of hepatocellular carcinoma at 1.5 T using the liver imaging reporting and data system (LI-RADS v.2017). Cancer Imaging, 2018, 18, 48.	1.2	15
33	Quantitative perfusion imaging of neoplastic liver lesions: A multi-institution study. Scientific Reports, 2018, 8, 4990.	1.6	14
34	Consensus report from the 9th International Forum for Liver Magnetic Resonance Imaging: applications of gadoxetic acid-enhanced imaging. European Radiology, 2021, 31, 5615-5628.	2.3	14
35	Magnetic resonance imaging and diffusion-weighted imaging-based histogram analyses in predicting glypican 3-positive hepatocellular carcinoma. European Journal of Radiology, 2021, 139, 109732.	1.2	14
36	Simultaneous multitarget radiotherapy using helical tomotherapy and its combination with sorafenib for pulmonary metastases from hepatocellular carcinoma. Oncotarget, 2016, 7, 48586-48599.	0.8	14

#	Article	IF	CITATIONS
37	Diffusion kurtosis imaging for the assessment of renal fibrosis of chronic kidney disease: A preliminary study. Magnetic Resonance Imaging, 2021, 80, 113-120.	1.0	13
38	Dynamic contrast-enhanced (DCE) MRI assessment of microvascular characteristics in the murine orthotopic pancreatic cancer model. Magnetic Resonance Imaging, 2015, 33, 737-760.	1.0	12
39	A comparative study of MR extracellular volume fraction measurement and two-dimensional shear-wave elastography in assessment of liver fibrosis with chronic hepatitis B. Abdominal Radiology, 2019, 44, 1407-1414.	1.0	12
40	Recurrence After Curative Resection of Hepatitis B Virus–Related Hepatocellular Carcinoma: Diagnostic Algorithms on Gadoxetic Acid–Enhanced Magnetic Resonance Imaging. Liver Transplantation, 2020, 26, 751-763.	1.3	12
41	Preliminary Exploration of the Application of Vesical <scp>Imagingâ€Reporting</scp> and Data System ( <scp>Vlâ€RADS</scp> ) in Postâ€treatment Patients With Bladder Cancer: A Prospective Singleâ€Center Study. Journal of Magnetic Resonance Imaging, 2022, 55, 275-286.	1.9	12
42	Preliminary Experience of 5.0 T Higher Field Abdominal Diffusionâ€Weighted <scp>MRI</scp> : Agreement of Apparent Diffusion Coefficient With 3.0 T Imaging. Journal of Magnetic Resonance Imaging, 2022, 56, 1009-1017.	1.9	12
43	A Multi-Parametric Radiomics Nomogram for Preoperative Prediction of Microvascular Invasion Status in Intrahepatic Cholangiocarcinoma. Frontiers in Oncology, 2022, 12, 838701.	1.3	11
44	MR imaging of hepatocellular adenomas on genotype-phenotype classification: A report from China. European Journal of Radiology, 2018, 100, 135-141.	1.2	10
45	Comparative study of evaluating the microcirculatory function status of primary small HCC between the CE (DCE-MRI) and Non-CE (IVIM-DWI) MR Perfusion Imaging. Abdominal Radiology, 2021, 46, 2575-2583.	1.0	10
46	Detecting the muscle invasiveness of bladder cancer: An application of diffusion kurtosis imaging and tumor contact length. European Journal of Radiology, 2022, 151, 110329.	1.2	10
47	Association of Aortic Compliance and Brachial Endothelial Function with Cerebral Small Vessel Disease in Type 2 Diabetes Mellitus Patients: Assessment with High-Resolution MRI. BioMed Research International, 2016, 2016, 1-8.	0.9	9
48	ADC similarity predicts microvascular invasion of bifocal hepatocellular carcinoma. Abdominal Radiology, 2018, 43, 2295-2302.	1.0	9
49	Value of MRI morphologic features with pT1â€⊋ rectal cancer in determining lymph node metastasis. Journal of Surgical Oncology, 2018, 118, 544-550.	0.8	9
50	Functional network changes in the hippocampus contribute to depressive symptoms in epilepsy. Seizure: the Journal of the British Epilepsy Association, 2018, 60, 16-22.	0.9	9
51	Additional value of MRI-detected EMVI scoring system in rectal cancer: applicability in predicting synchronous metastasis. Tumori, 2020, 106, 286-294.	0.6	9
52	Prospective comparison of integrated on-site CT-fractional flow reserve and static CT perfusion with coronary CT angiography for detection of flow-limiting coronary stenosis. European Radiology, 2021, 31, 5096-5105.	2.3	9
53	A <scp>Multiparametric</scp> Fusion Deep Learning Model Based on <scp>DCEâ€MRI</scp> for Preoperative Prediction of Microvascular Invasion in Intrahepatic Cholangiocarcinoma. Journal of Magnetic Resonance Imaging, 2022, 56, 1029-1039.	1.9	9
54	Image quality of automatic coronary CT angiography reconstruction for patients with HR ≥ 75Âbpm using an Al-assisted 16-cm z-coverage CT scanner. BMC Medical Imaging, 2021, 21, 24.	1.4	8

#	Article	IF	CITATIONS
55	Staging Chronic Hepatitis B Related Liver Fibrosis with a Fractional Order Calculus Diffusion Model. Academic Radiology, 2022, 29, 951-963.	1.3	8
56	Modified Subtraction Coronary CT Angiography with a Two-Breathhold Technique: Image Quality and Diagnostic Accuracy in Patients with Coronary Calcifications. Korean Journal of Radiology, 2019, 20, 1146.	1.5	8
57	MRI-based Nomogram Predicts the Risk of Progression of Unresectable Hepatocellular Carcinoma After Combined Lenvatinib and anti-PD-1 Antibody Therapy. Academic Radiology, 2022, 29, 819-829.	1.3	8
58	Whole-tumour evaluation with MRI and radiomics features to predict the efficacy of S-1 for adjuvant chemotherapy in postoperative pancreatic cancer patients: a pilot study. BMC Medical Imaging, 2021, 21, 75.	1.4	7
59	Assessment of Non-contrast-enhanced Dixon Water-fat Separation Compressed Sensing Whole-heart Coronary MR Angiography at 3.0 T: A Single-center Experience. Academic Radiology, 2022, 29, S82-S90.	1.3	7
60	Radiomics on Gadoxetate Disodium-enhanced MRI: Non-invasively Identifying Glypican 3-Positive Hepatocellular Carcinoma and Postoperative Recurrence. Academic Radiology, 2023, 30, 49-63.	1.3	7
61	The combined effect of hypertension and type 2 diabetes mellitus on aortic stiffness and endothelial dysfunction: An integrated study with high-resolution MRI. Magnetic Resonance Imaging, 2014, 32, 211-216.	1.0	6
62	Coronary Artery Plaque Imaging. Current Atherosclerosis Reports, 2017, 19, 37.	2.0	6
63	Non-contrast-enhanced MR angiography in the diagnosis of Budd-Chiari syndrome (BCS) compared with digital subtraction angiography (DSA): Preliminary results. Magnetic Resonance Imaging, 2017, 36, 7-11.	1.0	6
64	Assessment of thoracic vasculature in patients with central bronchogenic carcinoma by unenhanced magnetic resonance angiography: comparison between 2D free-breathing TrueFISP, 2D breath-hold TrueFISP and 3D respiratory-triggered SPACE. Journal of Thoracic Disease, 2017, 9, 1624-1633.	0.6	6
65	Clinical Application of Nonâ€Contrastâ€Enhanced Dixon Waterâ€Fat Separation Compressed <scp>SENSE</scp> Wholeâ€Heart Coronary <scp>MR</scp> Angiography at 3.0ÂT With and Without Nitroglycerin. Journal of Magnetic Resonance Imaging, 2022, 55, 579-591.	1.9	6
66	Quantification of myocardial hemorrhage using T2* cardiovascular magnetic resonance at 1.5T with ex-vivo validation. Journal of Cardiovascular Magnetic Resonance, 2021, 23, 104.	1.6	6
67	Grade 2 pancreatic neuroendocrine tumors: overbroad scope of Ki-67 index according to MRI features. Abdominal Radiology, 2018, 43, 3016-3024.	1.0	5
68	RAF1 expression is correlated with HAF, a parameter of liver computed tomographic perfusion, and may predict the early therapeutic response to sorafenib in advanced hepatocellular carcinoma patients. Open Medicine (Poland), 2020, 15, 167-174.	0.6	5
69	Liver computed tomographic perfusion for monitoring the early therapeutic response to sorafenib in advanced hepatocellular carcinoma patients. Journal of Cancer Research and Therapeutics, 2018, 14, 1556.	0.3	5
70	Radiomics Based on Contrast-Enhanced MRI in Differentiation Between Fat-Poor Angiomyolipoma and Hepatocellular Carcinoma in Noncirrhotic Liver: A Multicenter Analysis. Frontiers in Oncology, 2021, 11, 744756.	1.3	5
71	Apparent Diffusion Coefficient <scp>MRI</scp> Shows Association With Early Progression of Unresectable Intrahepatic Cholangiocarcinoma With Combined Targetedâ€Immunotherapy. Journal of Magnetic Resonance Imaging, 2023, 57, 275-284.	1.9	5
72	Optimization of MR diffusion-weighted imaging acquisitions for pancreatic cancer at 3.0T. Magnetic Resonance Imaging, 2014, 32, 875-879.	1.0	4

#	Article	IF	CITATIONS
73	Coronary Microembolization with Normal Epicardial Coronary Arteries and No Visible Infarcts on Nitrobluetetrazolium Chloride-Stained Specimens: Evaluation with Cardiac Magnetic Resonance Imaging in a Swine Model. Korean Journal of Radiology, 2016, 17, 83.	1.5	4
74	S100A4 overexpression in pancreatic ductal adenocarcinoma: imaging biomarkers from whole-tumor evaluation with MRI and texture analysis. Abdominal Radiology, 2021, 46, 623-635.	1.0	4
75	T 1 Mapping on Gdâ€EOBâ€DTPA â€Enhanced MRI for the Prediction of Oxaliplatinâ€Induced Liver Injury in a Mouse Model. Journal of Magnetic Resonance Imaging, 2021, 53, 896-902.	1.9	4
76	Role of free-breathing motion-corrected late gadolinium enhancement technique for image quality assessment and LGE quantification. European Journal of Radiology, 2021, 135, 109510.	1.2	4
77	A Semi-Automatic Step-by-Step Expert-Guided LI-RADS Grading System Based on Gadoxetic Acid-Enhanced MRI. Journal of Hepatocellular Carcinoma, 2021, Volume 8, 671-683.	1.8	4
78	Assessment of intramyocardial hemorrhage with dark-blood T2*-weighted cardiovascular magnetic resonance. Journal of Cardiovascular Magnetic Resonance, 2021, 23, 88.	1.6	4
79	Contrast-enhanced magnetic resonance imaging perfusion can predict microvascular invasion in patients with hepatocellular carcinoma (between 1 and 5Âcm). Abdominal Radiology, 2022, 47, 3264-3275.	1.0	4
80	Contrast-enhanced MRI could predict response of systemic therapy in advanced intrahepatic cholangiocarcinoma. European Radiology, 2022, 32, 5156-5165.	2.3	4
81	Tumor contour irregularity on preoperative imaging: a practical and useful prognostic parameter for papillary renal cell carcinoma. European Radiology, 2021, 31, 3745-3753.	2.3	3
82	Artificial intelligence study on left ventricular function among normal individuals, hypertrophic cardiomyopathy and dilated cardiomyopathy patients using 1.5T cardiac cine MR images obtained by SSFP sequence. British Journal of Radiology, 2022, 95, 20201060.	1.0	3
83	Application of MSCT characteristic nomogram model in predicting invasion of pancreatic solid pseudopapillary neoplasms. European Journal of Radiology, 2022, 149, 110201.	1.2	3
84	MR imaging of primary hepatic neuroendocrine neoplasm and metastatic hepatic neuroendocrine neoplasm: a comparative study. Radiologia Medica, 2015, 120, 1012-1020.	4.7	2
85	Gd-EOB-DTPA-enhanced MR findings in chemotherapy-induced sinusoidal obstruction syndrome in colorectal liver metastases. Journal of International Medical Research, 2020, 48, 030006052092603.	0.4	2
86	Free-breathing BLADE acquisition method improves T2-weighted cardiac MR image quality compared with conventional breath-hold turbo spin-echo cartesian acquisition. Acta Radiologica, 2021, 62, 341-347.	0.5	2
87	Early changes in intravoxel incoherent motion MRI parameters can potentially predict response to chemoradiotherapy in rectal cancer: An animal study. Magnetic Resonance Imaging, 2021, 78, 52-57.	1.0	2
88	Automatic vs manual coronary CT angiography reconstruction for whole-heart coverage CT scanner: a comparison study in general patient population. Journal of X-Ray Science and Technology, 2022, 30, 389-398.	0.7	2
89	Clinical study of digital mammography, contrast-enhanced MRI as well as their combination in the diagnosis of breast cancer. Chinese-German Journal of Clinical Oncology, 2008, 7, 286-291.	0.1	1
90	Comparative study between MRI features and pathology in FIGO stage I and II endometrial carcinoma. Chinese-German Journal of Clinical Oncology, 2006, 5, 209-212.	0.1	0

#	Article	IF	CITATIONS
91	Reply: Prediction of the Left Ventricular Functional Outcome by Myocardial Extracellular Volume Fraction Measured Using Magnetic Resonance Imaging; Methodological Issue. Korean Journal of Radiology, 2019, 20, 1311.	1.5	о
92	Detecting Regional Fibrosis in Hypertrophic Cardiomyopathy: The Utility of Myocardial Strain Based on Cardiac Magnetic Resonance. Academic Radiology, 2022, , .	1.3	0